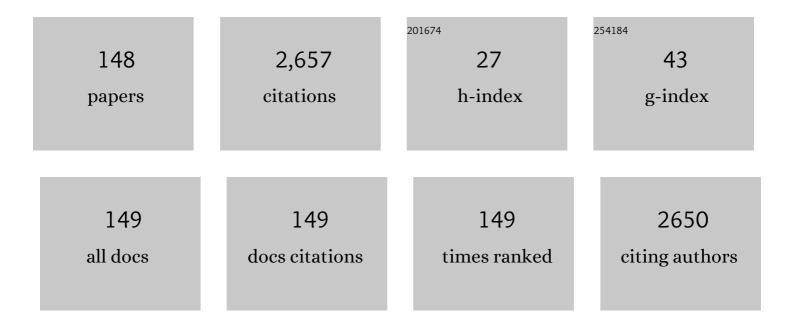
## Jian Zhang Chen

List of Publications by Year in descending order

Source: https://exaly.com/author-pdf/2908011/publications.pdf Version: 2024-02-01



#	Article	IF	CITATIONS
1	Capacitive sensing of droplets for microfluidic devices based on thermocapillary actuation. Lab on A Chip, 2004, 4, 473.	6.0	143
2	Effect of contact angle hysteresis on thermocapillary droplet actuation. Journal of Applied Physics, 2005, 97, 014906.	2.5	124
3	All-vanadium redox flow batteries with graphite felt electrodes treated by atmospheric pressure plasma jets. Journal of Power Sources, 2015, 274, 894-898.	7.8	113
4	Enhanced Thermoelectric Power in Dual-Gated Bilayer Graphene. Physical Review Letters, 2011, 107, 186602.	7.8	74
5	Two dimensional electron gases in polycrystalline MgZnO/ZnO heterostructures grown by rf-sputtering process. Journal of Applied Physics, 2010, 108, .	2.5	71
6	Preparation of nanoporous TiO2 films for DSSC application by a rapid atmospheric pressure plasma jet sintering process. Journal of Power Sources, 2013, 234, 16-22.	7.8	71
7	Rapid Atmospheric Pressure Plasma Jet Processed Reduced Graphene Oxide Counter Electrodes for Dye-Sensitized Solar Cells. ACS Applied Materials & Interfaces, 2014, 6, 15105-15112.	8.0	71
8	Ultrafast synthesis of carbon-nanotube counter electrodes for dye-sensitized solar cells using an atmospheric-pressure plasma jet. Carbon, 2016, 98, 34-40.	10.3	59
9	Improved performance of polyaniline/reduced-graphene-oxide supercapacitor using atmospheric-pressure-plasma-jet surface treatment of carbon cloth. Electrochimica Acta, 2018, 260, 391-399.	5.2	58
10	Feasibility study of surface-modified carbon cloth electrodes using atmospheric pressure plasma jets for microbial fuel cells. Journal of Power Sources, 2016, 336, 99-106.	7.8	56
11	Crystallization temperature and activation energy of rf-sputtered near-equiatomic TiNi and Ti50Ni40Cu10 thin films. Journal of Non-Crystalline Solids, 2001, 288, 159-165.	3.1	53
12	Mobility Enhancement of Polycrystalline MgZnO/ZnO Thin Film Layers With Modulation Doping and Polarization Effects. IEEE Transactions on Electron Devices, 2010, 57, 696-703.	3.0	51
13	Dye-sensitized solar cells with nanoporous TiO2 photoanodes sintered by N2 and air atmospheric pressure plasma jets with/without air-quenching. Journal of Power Sources, 2014, 251, 215-221.	7.8	50
14	Atmospheric pressure plasma jet processed nanoporous Fe2O3/CNT composites for supercapacitor application. Journal of Alloys and Compounds, 2016, 676, 469-473.	5.5	48
15	Crystallization behavior of r.fsputtered TiNi thin films. Thin Solid Films, 1999, 339, 194-199.	1.8	42
16	Atmospheric-pressure-plasma-jet processed carbon nanotube (CNT)–reduced graphene oxide (rGO) nanocomposites for gel-electrolyte supercapacitors. RSC Advances, 2018, 8, 2851-2857.	3.6	41
17	Atmospheric-pressure plasma jet processed SnO2/CNT nanocomposite for supercapacitor application. Ceramics International, 2016, 42, 14287-14291.	4.8	40
18	Positive Gate-Bias Temperature Stability of RF-Sputtered \$hbox{Mg}_{0.05}hbox{Zn}_{0.95}hbox{O}\$ Active-Layer Thin-Film Transistors. IEEE Transactions on Electron Devices, 2012, 59, 151-158.	3.0	37

#	Article	IF	CITATIONS
19	Sol–gel derived amorphous/nanocrystalline MgZnO thin films annealed by atmospheric pressure plasma jets. Ceramics International, 2014, 40, 2707-2715.	4.8	35
20	Oxygen-deficient indium tin oxide thin films annealed by atmospheric pressure plasma jets with/without air-quenching. Applied Surface Science, 2014, 292, 213-218.	6.1	35
21	Atmospheric pressure plasma jet processed reduced graphene oxides for supercapacitor application. Journal of Alloys and Compounds, 2017, 692, 558-562.	5.5	35
22	A study of mixing in thermocapillary flows on micropatterned surfaces. Philosophical Transactions Series A, Mathematical, Physical, and Engineering Sciences, 2004, 362, 1037-1058.	3.4	34
23	Application of atmospheric-pressure plasma jet processed carbon nanotubes to liquid and quasi-solid-state gel electrolyte supercapacitors. Applied Surface Science, 2017, 425, 321-328.	6.1	34
24	Bandgap tuning of MgZnO in flexible transparent n+-ZnO:Al/n-MgZnO/p-CuAlOx:Ca diodes on polyethylene terephthalate substrates. Journal of Alloys and Compounds, 2012, 544, 111-114.	5.5	32
25	Rapid Atmospheric-Pressure-Plasma-Jet Processed Porous Materials for Energy Harvesting and Storage Devices. Coatings, 2015, 5, 26-38.	2.6	31
26	Reliability of Active-Matrix Organic Light-Emitting-Diode Arrays With Amorphous Silicon Thin-Film Transistor Backplanes on Clear Plastic. IEEE Electron Device Letters, 2008, 29, 63-66.	3.9	30
27	Influence of rapid-thermal-annealing temperature on properties of rf-sputtered SnOx thin films. Applied Surface Science, 2015, 327, 358-363.	6.1	27
28	UV photocurrent responses of ZnO and MgZnO/ZnO processed by atmospheric pressure plasma jets. Journal of Alloys and Compounds, 2015, 628, 68-74.	5.5	26
29	Atmospheric-Pressure Plasma Jet Processed Pt-Decorated Reduced Graphene Oxides for Counter-Electrodes of Dye-Sensitized Solar Cells. Coatings, 2016, 6, 44.	2.6	25
30	Electrical properties of modulation-doped rf-sputtered polycrystalline MgZnO/ZnO heterostructures. Journal Physics D: Applied Physics, 2011, 44, 455101.	2.8	24
31	Enhanced optical absorption of dye-sensitized solar cells with microcavity-embedded TiO_2 photoanodes. Optics Express, 2012, 20, A168.	3.4	24
32	Flexible Transparent ZnO:Al/ZnO/CuAlO x :Ca Heterojunction Diodes on Polyethylene Terephthalate Substrates. Journal of Electronic Materials, 2013, 42, 1242-1245.	2.2	24
33	Atmospheric pressure plasma jet annealed ZnO films for MgZnO/ZnO heterojunctions. Journal Physics D: Applied Physics, 2013, 46, 075202.	2.8	24
34	Surface modification of carbon cloth anodes for microbial fuel cells using atmospheric-pressure plasma jet processed reduced graphene oxides. RSC Advances, 2017, 7, 56433-56439.	3.6	24
35	Atmospheric-pressure plasma jet processed Pt/ZnO composites and its application as counter-electrodes for dye-sensitized solar cells. Applied Surface Science, 2018, 436, 690-696.	6.1	24
36	Nitrogen DC-pulse atmospheric-pressure-plasma jet (APPJ)-processed reduced graphene oxide (rGO)â€ʿcarbon black (CB) nanocomposite electrodes for supercapacitor applications. Diamond and Related Materials, 2018, 88, 23-31.	3.9	24

#	Article	IF	CITATIONS
37	Deposition of transparent and conductive ZnO films by an atmospheric pressure plasma-jet-assisted process. Thin Solid Films, 2014, 570, 423-428.	1.8	23
38	Silver halide fiber-based evanescent-wave liquid droplet sensing with room temperature mid-infrared quantum cascade lasers. Optics Express, 2005, 13, 5953.	3.4	22
39	MgZnO/ZnO Heterostructure Field-Effect Transistors Fabricated by RF-Sputtering. ECS Transactions, 2013, 50, 83-93.	0.5	22
40	Flexible reduced graphene oxide supercapacitor fabricated using a nitrogen dc-pulse atmospheric-pressure plasma jet. Materials Research Express, 2017, 4, 025504.	1.6	22
41	Tyrosinase/Chitosan/Reduced Graphene Oxide Modified Screen-Printed Carbon Electrode for Sensitive and Interference-Free Detection of Dopamine. Applied Sciences (Switzerland), 2019, 9, 622.	2.5	22
42	Atmospheric-pressure-plasma-jet processed nanoporous TiO <sub>2</sub> photoanodes and Pt counter-electrodes for dye-sensitized solar cells. RSC Advances, 2015, 5, 45662-45667.	3.6	21
43	Nanohardness, corrosion and protein adsorption properties of CuAlO2 films deposited on 316L stainless steel for biomedical applications. Applied Surface Science, 2014, 289, 455-461.	6.1	20
44	Scan-Mode Atmospheric-Pressure Plasma Jet Processed Reduced Graphene Oxides for Quasi-Solid-State Gel-Electrolyte Supercapacitors. Coatings, 2018, 8, 52.	2.6	20
45	Feasibility study of atmospheric-pressure dielectric barrier discharge treatment on CH3NH3PbI3 films for inverted planar perovskite solar cells. Electrochimica Acta, 2019, 293, 1-7.	5.2	20
46	Improved performance of dye-sensitized solar cells with laser-textured nanoporous TiO2 photoanodes. Materials Letters, 2012, 66, 162-164.	2.6	19
47	O <sub>2</sub> /HMDSO-Plasma-Deposited Organic-Inorganic Hybrid Film for Gate Dielectric of MgZnO Thin-Film Transistor. Plasma Processes and Polymers, 2014, 11, 89-95.	3.0	19
48	Ultrafast atmospheric-pressure-plasma-jet processed conductive plasma-resistant Y 2 O 3 /carbon-nanotube nanocomposite. Journal of Alloys and Compounds, 2015, 651, 357-362.	5.5	19
49	In-situ atmospheric-pressure dielectric barrier discharge plasma treated CH3NH3PbI3 for perovskite solar cells in regular architecture. Applied Surface Science, 2019, 473, 468-475.	6.1	19
50	Atmospheric-Pressure-Plasma-Jet Particulate TiO2Scattering Layer Deposition Processes for Dye-Sensitized Solar Cells. ECS Journal of Solid State Science and Technology, 2014, 3, Q177-Q181.	1.8	18
51	Ultrafast synthesis of continuous Au thin films from chloroauric acid solution using an atmospheric pressure plasma jet. RSC Advances, 2015, 5, 99654-99657.	3.6	18
52	Low-Temperature (<40 °C) Atmospheric-Pressure Dielectric-Barrier-Discharge-Jet Treatment on Nickel Oxide for p–i–n Structure Perovskite Solar Cells. ACS Omega, 2020, 5, 6082-6089.	3.5	17
53	Flexible Complementary Oxide Thin-Film Transistor-Based Inverter With High Gain. IEEE Transactions on Electron Devices, 2021, 68, 1070-1074.	3.0	17
54	Effects of drain-bias and ambient on hump formation in the transfer curves of positively gate-biased MgZnO thin film transistors. Thin Solid Films, 2013, 529, 360-363.	1.8	16

#	Article	IF	CITATIONS
55	Single-layer organic–inorganic-hybrid thin-film encapsulation for organic solar cells. Journal Physics D: Applied Physics, 2013, 46, 435502.	2.8	16
56	Atmospheric-pressure-plasma-jet sintered nanoporous SnO2. Ceramics International, 2015, 41, 5478-5483.	4.8	16
57	Screen-printed SnO <sub>2</sub> /CNT quasi-solid-state gel-electrolyte supercapacitor. Materials Research Express, 2017, 4, 115501.	1.6	16
58	Dielectric Barrier Discharge Plasma Jet (DBDjet) Processed Reduced Graphene Oxide/Polypyrrole/Chitosan Nanocomposite Supercapacitors. Polymers, 2021, 13, 3585.	4.5	16
59	Electrical, optical, and microstructural properties of sol–gel derived HfZnO thin films. Journal of Alloys and Compounds, 2014, 601, 223-230.	5.5	14
60	SnO2/CNT nanocomposite supercapacitors fabricated using scanning atmospheric-pressure plasma jets. Materials Research Express, 2016, 3, 085002.	1.6	14
61	Flexible quasi-solid-state SnO2/CNT supercapacitor processed by a dc-pulse nitrogen atmospheric-pressure plasma jet. Journal of Energy Storage, 2017, 11, 237-241.	8.1	14
62	Atmospheric-Pressure Plasma Jet Processed Carbon-Based Electrochemical Sensor Integrated with a 3D-Printed Microfluidic Channel. Journal of the Electrochemical Society, 2017, 164, B534-B541.	2.9	14
63	Electropolymerized Poly(3,4-ethylenedioxythiophene)/Screen-Printed Reduced Graphene Oxide–Chitosan Bilayer Electrodes for Flexible Supercapacitors. ACS Omega, 2021, 6, 16455-16464.	3.5	14
64	Chemical machined thin foils of TiNi shape memory alloy. Materials Chemistry and Physics, 1999, 58, 162-165.	4.0	13
65	Negative bias temperature instability of Rf-sputtered Mg <sub>0.05</sub> Zn <sub>0.95</sub> O thin film transistors with MgO gate dielectrics. Semiconductor Science and Technology, 2011, 26, 105007.	2.0	13
66	Phase transitions of room temperature RF-sputtered ZnO/Mg0.4Zn0.6O multilayer thin films after thermal annealing. Thin Solid Films, 2012, 520, 1918-1923.	1.8	13
67	Atmospheric-pressure-plasma-jet sintered dual-scale porous TiO 2 using an economically favorable NaCl solution. Journal of Power Sources, 2015, 281, 252-257.	7.8	13
68	Influence of Ca/Al Ratio on Properties of Amorphous/Nanocrystalline Cu–Al–Ca–O Thin Films. Journal of the American Ceramic Society, 2015, 98, 125-129.	3.8	13
69	Low-Temperature-Annealed Reduced Graphene Oxide–Polyaniline Nanocomposites for Supercapacitor Applications. Journal of Electronic Materials, 2018, 47, 3861-3868.	2.2	13
70	Flexible rGO-SnO2 supercapacitors converted from pastes containing SnCl2 liquid precursor using atmospheric-pressure plasma jet. Ceramics International, 2021, 47, 1651-1659.	4.8	13
71	KrF excimer laser irradiated nanoporous TiO 2 layers for dye-sensitized solar cells: Influence of laser power density. Ceramics International, 2013, 39, 6183-6188.	4.8	12
72	Electromechanical properties of MgZnO/ZnO heterostructures on flexible polyimide and stainless steel substrates under flexing. Journal Physics D: Applied Physics, 2014, 47, 255102.	2.8	12

#	Article	IF	CITATIONS
73	Influence of annealing temperature on properties of room-temperature rf-sputtered CuAlOx:Ca thin films. Thin Solid Films, 2014, 550, 591-594.	1.8	12
74	Abnormal temperature-dependent stability of on-plastic a-Si:H thin film transistors fabricated at 150 °C. Journal of Applied Physics, 2008, 104, 044508.	2.5	11
75	Enhanced Photoelectrochemical Performance of Photoanode Fabricated Using Polystyrene Ball Embedded TiO[sub 2] Pastes. Electrochemical and Solid-State Letters, 2011, 14, B6.	2.2	11
76	Two dimensional thermoelectric platforms for thermocapillary droplet actuation. RSC Advances, 2012, 2, 1639-1642.	3.6	11
77	Transitions of bandgap and built-in stress for sputtered HfZnO thin films after thermal treatments. Journal of Applied Physics, 2013, 114, .	2.5	11
78	Dielectric-Barrier-Discharge Jet Treated Flexible Supercapacitors with Carbon Cloth Current Collectors of Long-Lasting Hydrophilicity. Journal of the Electrochemical Society, 2020, 167, 116511.	2.9	11
79	DC-pulse atmospheric-pressure plasma jet and dielectric barrier discharge surface treatments on fluorine-doped tin oxide for perovskite solar cell application. Journal Physics D: Applied Physics, 2018, 51, 025502.	2.8	10
80	Composition control of r.fsputtered Ti50Ni40Cu10 thin films using optical emission spectroscopy. Thin Solid Films, 2000, 365, 61-66.	1.8	9
81	An Unsupervised Approach to Cluster Web Search Results Based on Word Sense Communities. , 2008, , .		9
82	Periodic anti-ring back reflectors for hydrogenated amorphous silicon thin-film solar cells. Optics Express, 2014, 22, A1128.	3.4	9
83	Effect of Al/Cu ratios on the optical, electrical, and electrochemical properties of Cu–Al–Ca–O thin films. Journal of Alloys and Compounds, 2014, 609, 111-115.	5.5	9
84	A Photoactivated Gas Detector for Toluene Sensing at Room Temperature Based on New Coral-Like ZnO Nanostructure Arrays. Sensors, 2016, 16, 1820.	3.8	9
85	A Comparison Study of Furnace and Atmospheric-Pressure-Plasma Jet Calcined Pt-Decorated Reduced Graphene Oxides for Dye-Sensitized Solar Cell Application. Journal of the Electrochemical Society, 2017, 164, H931-H935.	2.9	9
86	Carbon Dioxide Tornado-Type Atmospheric-Pressure-Plasma-Jet-Processed rGO-SnO2 Nanocomposites for Symmetric Supercapacitors. Materials, 2021, 14, 2777.	2.9	9
87	Facile method to convert petal effect surface to lotus effect surface for superhydrophobic polydimethylsiloxane. Surfaces and Interfaces, 2022, 30, 101901.	3.0	9
88	The Electromechanical Characteristics of ZnO Grown on Poly(ethylene terephthalate) Substrates. Journal of the Electrochemical Society, 2010, 157, H750.	2.9	8
89	Ultrafast Atmospheric-Pressure-Plasma-Jet Sintering of Nanoporous TiO <sub>2</sub> -SnO <sub>2</sub> Composites with Features Defined by Screen-Printing. ECS Journal of Solid State Science and Technology, 2015, 4, P3020-P3025.	1.8	8
90	Optoelectronic properties of infrared rapid-thermal-annealed SnOx thin films. Ceramics International, 2015, 41, 13502-13508.	4.8	8

#	Article	IF	CITATIONS
91	Dielectric barrier discharge jet processed TiO <sub>2</sub> nanoparticle layer for flexible perovskite solar cells. Journal Physics D: Applied Physics, 2022, 55, 034003.	2.8	8
92	Direct liquid cooling of room-temperature operated quantum cascade lasers. Electronics Letters, 2006, 42, 534.	1.0	7
93	Dynamically programmable surface micro-wrinkles on PDMS-SMA composite. Smart Materials and Structures, 2014, 23, 115007.	3.5	7
94	Atmospheric-pressure surface-diffusion dielectric-barrier discharge (SDDBD) plasma surface modification of PEDOT:PSS. Synthetic Metals, 2019, 256, 116114.	3.9	7
95	Stability of Amorphous Silicon Thin Film Transistors under Prolonged High Compressive Strain. Materials Research Society Symposia Proceedings, 2007, 989, 4.	0.1	6
96	Deposition of ZnO Thin Films by an Atmospheric Pressure Plasma Jet-Assisted Process: The Selection of Precursors. IEEE Transactions on Plasma Science, 2015, 43, 670-674.	1.3	6
97	Atmospheric-pressure-plasma-jet sintered nanoporous AlN/CNT composites. Applied Surface Science, 2016, 377, 75-80.	6.1	6
98	Time Evolution Characterization of Atmospheric-Pressure Plasma Jet (APPJ)-Synthesized Pt-SnOx Catalysts. Metals, 2018, 8, 690.	2.3	6
99	Conversion of dense and continuous nickel oxide compound thin films using nitrogen DC-pulse atmospheric-pressure plasma jet. Ceramics International, 2019, 45, 22078-22084.	4.8	6
100	Hydrophilic patterning of octadecyltrichlorosilane (OTS)-coated paper via atmospheric-pressure dielectric-barrier-discharge jet (DBDjet). Cellulose, 2020, 27, 10293-10301.	4.9	6
101	Low Temperature (<40 °C) Atmospheric-Pressure Dielectric-Barrier-Discharge-jet (DBDjet) Plasma Treatment on Jet-Sprayed Silver Nanowires (AgNWs) Electrodes for Fully Solution-Processed n-i-p Structure Perovskite Solar Cells. ECS Journal of Solid State Science and Technology, 2020, 9, 055016.	1.8	6
102	Scanning atmospheric-pressure plasma jet treatment of nickel oxide with peak temperature of â^¼500 °C for fabricating p–i–n structure perovskite solar cells. RSC Advances, 2020, 10, 11166-11172.	3.6	6
103	Comparison between atmospheric-pressure-plasma-jet-processed and furnace-calcined rGO-MnOx nanocomposite electrodes for gel-electrolyte supercapacitors. Journal of Alloys and Compounds, 2022, 911, 165006.	5.5	6
104	Plasma-etched nanoporous TiO <sub>2</sub> using Ag nanoparticle masks: application for photoanodes of dye-sensitized solar cells. Materials Research Express, 2014, 1, 025505.	1.6	5
105	Nitrogen Atmospheric-Pressure-Plasma-Jet Induced Oxidation of SnOx Thin Films. Plasma Chemistry and Plasma Processing, 2015, 35, 979-991.	2.4	5
106	Ar dielectric barrier discharge jet (DBDjet) plasma treatment of reduced graphene oxide (rGO)–polyaniline (PANI)–chitosan (CS) nanocomposite on carbon cloth for supercapacitor application. Energy, Ecology and Environment, 2020, 5, 134-140.	3.9	5
107	Flexible reduced graphene oxide supercapacitors processed using atmospheric-pressure plasma jet under various temperatures adjusted by flow rate and jet-substrate distance. Materials Research Express, 2020, 7, 015602.	1.6	5
108	Electromechanical Stability of Flexible Nanocrystalline-Silicon Thin-Film Transistors. IEEE Electron Device Letters, 2010, 31, 222-224.	3.9	4

#	Article	IF	CITATIONS
109	Indium tin oxide sol–gel precursor conversion process using the third harmonics of Nd:YAG laser. Applied Surface Science, 2011, 257, 10042-10044.	6.1	4
110	Surface Modification of FeCoNiCr Medium-Entropy Alloy (MEA) Using Octadecyltrichlorosilane and Atmospheric-Pressure Plasma Jet. Polymers, 2020, 12, 788.	4.5	4
111	Improved efficiency and air stability of two-dimensional p-i-n inverted perovskite solar cells by Cs doping. RSC Advances, 2021, 11, 20200-20206.	3.6	4
112	Feasibility Study of Dielectric Barrier Discharge Jet-Patterned Perfluorodecyltrichlorosilane-Coated Paper for Biochemical Diagnosis. ECS Journal of Solid State Science and Technology, 2021, 10, 037005.	1.8	4
113	Characteristics of Graphite Felt Electrodes Treated by Atmospheric Pressure Plasma Jets for an All-Vanadium Redox Flow Battery. Materials, 2021, 14, 3847.	2.9	4
114	Low-Pressure Plasma-Processed Ruthenium/Nickel Foam Electrocatalysts for Hydrogen Evolution Reaction. Materials, 2022, 15, 2603.	2.9	4
115	Effects of SiN[sub x] Passivation and Gate Metal Roughness on the Performance of On-plastic a-Si:H TFTs. Electrochemical and Solid-State Letters, 2008, 11, H26.	2.2	3
116	Application of Atmospheric-Pressure-Plasma-Jet Modified Flexible Graphite Sheets in Reduced-Graphene-Oxide/Polyaniline Supercapacitors. Polymers, 2020, 12, 1228.	4.5	3
117	Atmospheric pressure plasma jet treatment enhances the effect of Alloy Primer on the bond strength between polymethyl methacrylate and stainless steels: application for retention of magnetic attachment to resin denture base. Colloids and Surfaces B: Biointerfaces, 2021, 197, 111440.	5.0	3
118	Silver mirror reaction metallized chromatography paper for supercapacitor application. Flexible and Printed Electronics, 2021, 6, 045010.	2.7	3
119	The Influence of Electromechanical Stress on the Stability of Nanocrystalline Silicon Thin Film Transistors Made on Colorless Polyimide Foil. ECS Transactions, 2010, 33, 65-69.	0.5	2
120	Influence of Annealing Conditions on the Bias Temperature Stability of MgZnO Thin Film Transistors. ECS Transactions, 2013, 50, 173-178.	0.5	2
121	Characterization of Hf/Mg co-doped ZnO thin films after thermal treatments. Thin Solid Films, 2014, 570, 457-463.	1.8	2
122	Oxidation of sputtered metallic Sn thin films using N <sub>2</sub> atmospheric pressure plasma jets. Materials Research Express, 2015, 2, 016504.	1.6	2
123	Electrochemical and Microstructural Investigations of PtFe Nanocompounds Synthesized by Atmospheric-Pressure Plasma Jet. Journal of the Electrochemical Society, 2020, 167, 056501.	2.9	2
124	Concentration effect on properties of Pt-NiOx nanocompounds converted from mixed chloroplatinic acid and nickel acetate precursor films using an atmospheric-pressure plasma jet. Journal of Applied Physics, 2020, 128, 043302.	2.5	2
125	Influence of mechanical bending strain on bias-stress stability of flexible top-gate p-type SnO TFTs. , 2020, , .		2

PbTiO<inf&gt;3&lt;/inf&gt;/P(VDF-TrFE) nanocomposites for flexible skin. , 2008, , .

1

#	Article	IF	CITATIONS
127	Effects of electro-mechanical stressing on the electrical characterization of on-plastic a-Si:H thin film transistors. Materials Research Society Symposia Proceedings, 2009, 1153, 1.	0.1	1
128	Dye-Sensitized Solar Cell with Photoanode Made with Polystyrene-Ball-Embedded TiO <sub>2</sub> Pastes. Japanese Journal of Applied Physics, 2011, 50, 06GF09.	1.5	1
129	Multi-layer thermoelectric-temperature-mapping microbial incubator designed for geo-biochemistry applications. Review of Scientific Instruments, 2012, 83, 045116.	1.3	1
130	Characterization of rf-sputtered HfMgZnO thin films. Materials Research Society Symposia Proceedings, 2012, 1432, 187.	0.1	1
131	Microstructural, electrical, and optical properties of sol–gel derived HfMgZnO thin films. Materials Research Express, 2015, 2, 096402.	1.6	1
132	Modeling and simulation of heat transfer characteristics of 12-inch wafer on electrostatic chuck. , 2015, , .		1
133	The Influence of Helium Dielectric Barrier Discharge Jet (DBDjet) Plasma Treatment on Bathocuproine (BCP) in p-i-n-Structure Perovskite Solar Cells. Polymers, 2021, 13, 4020.	4.5	1
134	East Asian Calligraphy Black Ink-Coated Paper as Flexible Conducting Electrode for Supercapacitor. ECS Journal of Solid State Science and Technology, 2021, 10, 123013.	1.8	1
135	Silver halide fiber-based evanescent-wave liquid droplet sensing with thermoelectrically cooled room temperature mid-infrared quantum cascade lasers. , 2005, 6010, 62.		Ο
136	Temperature and humidity effects on the stability of on-plastic a-Si:H thin film transistors with various conduction channel layer thicknesses. Materials Research Society Symposia Proceedings, 2008, 1066, 1.	0.1	0
137	Thermally Actuated Droplet Motion on Chemically Homogeneous, Striated, and Defected Surfaces. , 2008, , .		Ο
138	Influences of Polarization Effects in the Electrical Properties of Polycrystalline MgZnO/ZnO Heterostructure. Materials Research Society Symposia Proceedings, 2009, 1201, 90.	0.1	0
139	Mobility Study of Polycrystalline MgZnO/ZnO Thin Film Layers with Monte Carlo Method. , 2009, , .		Ο
140	DC and AC Gate-Bias Stability of Nanocrystalline Silicon Thin-Film Transistors Made on Colorless Polyimide Foil Substrates. Materials Research Society Symposia Proceedings, 2011, 1321, 259.	0.1	0
141	The effect of Zn/Sn Ratio on the Electrical Performance of Amorphous ZrZnSnO (ZZTO) Thin Film Transistors by RF Sputtering. ECS Transactions, 2013, 50, 185-189.	0.5	О
142	Back Cover: Plasma Process. Polym. 1â^•2014. Plasma Processes and Polymers, 2014, 11, 100-100.	3.0	0
143	Simulation studies on bipolar electrostatic chucks. , 2015, , .		0
144	HfZnO/ZnO Heterostructures Fabricated Using Low-Cost Large-Area Compatible Sputtering Processes. Materials Research Society Symposia Proceedings, 2015, 1731, 18.	0.1	0

#	Article	IF	CITATIONS
145	Rapid atmospheric-pressure-plasma processed nanomaterials for electrochemical energy harvesting and storage devices. , 2016, , .		0
146	Enhancement of gate-bias and current stress stability of P-type SnO thin-film transistors with SiN <inf>x</inf> /HfO <inf>2</inf> passivation layers. , 2016, , .		0
147	Investigation of ultrashort (< 1Âmin) calcination processes for conversion of Pt–SnOx from mixture of chloroplatinic acid and tin(II) chloride. SN Applied Sciences, 2019, 1, 1.	2.9	0
148	Plasmas Processes Applied on Metals and Alloys. Metals, 2020, 10, 349.	2.3	0